

# The Mechanistic Basis for Electronic Effects on Enantioselectivity in the (salen)Mn(III)-Catalyzed Epoxidation Reaction

Michael Palucki, Nathaniel S. Finney, Paul J. Pospisil, Mehmet L. Güler, Toyohisa Ishida, and Eric N. Jacobsen\*

Contribution from the Department of Chemistry and Chemical Biology, Harvard University, Cambridge, Massachusetts 02138

Received October 3, 1997

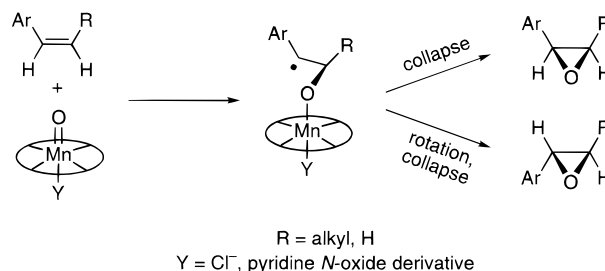
**Abstract:** Enantioselectivity in the (salen)Mn-catalyzed asymmetric epoxidation reaction correlates directly with the electronic properties of the ligand substituents, with complexes bearing electron-donating substituents affording highest ee's. Several lines of evidence point to a single factor—control of the position of the transition state along the reaction coordinate—as being responsible for the electronic effects on enantioselectivity. Analysis of the epoxidation of *cis*- $\beta$ -deuteriostyrene reveals that electron-rich catalysts display a more pronounced secondary inverse isotope effect than electron-deficient catalysts. A strong correlation between  $\Delta\Delta H^\ddagger$  and the electronic character of the catalyst is also observed. The conclusion that enantioselectivity is tied to the position of a transition state along the reaction coordinate may hold general implications for the design of asymmetric catalysts, particularly those that effect reactions without substrate precoordination.

## Introduction

Effective stereochemical communication between substrate and catalyst is essential for attaining high enantioselectivities in asymmetric catalytic reactions. Enzymatic processes achieve this, at least in part, by inducing substrate precoordination to catalyst prior to reaction, thereby minimizing the degrees of freedom in the critical transition state and maximizing selectivity-determining interactions between the catalyst's asymmetric environment and the substrate.<sup>1</sup> As might be anticipated, many of the most successful nonenzymatic asymmetric catalyst systems also operate on this principle: archetypal examples of such effective substrate-directed catalytic reactions<sup>2</sup> include rhodium-catalyzed asymmetric hydrogenation,<sup>3</sup> the Sharpless epoxidation of allylic alcohols,<sup>4</sup> and the Noyori Ru(BINAP)-catalyzed hydrogenation of functionalized olefins and ketones.<sup>5</sup>

In contrast to this enzymatic motif, a number of practical and effective asymmetric catalyst systems have been discovered that do not require a specific precoordinating group in the substrate in order to impart high enantioselectivities.<sup>6</sup> Such systems offer the potential advantage of enhanced generality, with reaction scope limited only by the nature of the functional-

## Scheme 1



ity undergoing transformation. The (salen)Mn-catalyzed olefin epoxidation is among the most useful and widely applicable reactions that do not involve substrate precoordination.<sup>6b</sup> With the appropriate choice of ligand and reaction conditions, it has proven effective for virtually every class of unfunctionalized conjugated olefin.<sup>7</sup> Scheme 1 illustrates the simplest mechanism for this reaction which is consistent with the available data. In this reaction epoxidation proceeds through two sequential C–O bond-forming steps: addition of substrate alkene to a (salen)-Mn(V) oxo species generates a radical intermediate, which in turn partitions between collapse and rotation/collapse processes to provide the observed mixture of *cis* and *trans* epoxides.<sup>8</sup>

In 1991, we reported the observation of dramatic catalyst electronic effects on the enantioselectivity of (salen)Mn-

(1) Walsh, C. *Enzymatic Reaction Mechanisms*; W. H. Freeman and Company: New York, 1979.

(2) For a definitive discussion of substrate-directed reactions, see: (a) Hoveyda, A. H.; Evans, D. A.; Fu, G. C. *Chem. Rev. (Washington, D.C.)* **1993**, *93*, 1307.

(3) Halpern, J. *Science* **1982**, *217*, 401.

(4) Johnson, R. A.; Sharpless, K. B. In *Catalytic Asymmetric Synthesis*; Ojima, I., Ed.; VCH: New York, 1993; Chapter 4.1.

(5) Takaya, H.; Ohta, T.; Noyori, R. In *Catalytic Asymmetric Synthesis*; Ojima, I., Ed.; VCH: New York, 1993; Chapter 1.

(6) For example, asymmetric dihydroxylation: (a) Kolb, H. C.; Van-Nieuwenhze, M. S.; Sharpless, K. B. *Chem. Rev. (Washington, D.C.)* **1994**, *94*, 2483. Asymmetric epoxidation: (b) Jacobsen, E. N. In *Catalytic Asymmetric Synthesis*; Ojima, I., Ed.; VCH: New York, 1993; Chapter 4.2. Asymmetric aziridination: (c) Li, Z.; Conser, K. R.; Jacobsen, E. N. *J. Am. Chem. Soc.* **1993**, *115*, 5326. (d) Evans, D. A.; Faul, M. M.; Bilodeau, M. T.; Anderson, B. A.; Barnes, D. M. *J. Am. Chem. Soc.* **1993**, *115*, 5328. Asymmetric cyclopropanation: Doyle, M. P. In *Catalytic Asymmetric Synthesis*; Ojima, I., Ed.; VCH: New York, 1993; Chapter 3.

(7) (a) Jacobsen, E. N. In *Comprehensive Organometallic Chemistry II*; Wilkinson, G.; Stone, F. G. A.; Abel, E. W., Hegedus, L. S., Eds.; Pergamon: New York, 1995; Vol. 12, Chapter 11.1. (b) Katsuki, T. *Coord. Chem. Rev.* **1995**, *140*, 189.

(8) (a) Finney, N. S.; Pospisil, P. J.; Chang, S.; Palucki, M.; Konsler, R. G.; Hansen, K. B.; Jacobsen, E. N. *Angew. Chem., Int. Ed. Engl.* **1997**, *36*, 1720. (b) Jacobsen, E. N.; Deng, L.; Furukawa, Y.; Martínez, L. E. *Tetrahedron* **1994**, *50*, 4323. (c) Hosoya, N.; Hatayama, A.; Yanai, K.; Fujii, H.; Irie, R.; Katsuki, T. *Synlett.* **1993**, 641. (d) Srinivasan, K.; Michaud, P.; Kochi, J. K. *J. Am. Chem. Soc.* **1986**, *108*, 2309. For an alternative mechanistic interpretation, see: (e) Linde, C.; Arnold, M.; Norrby, P.-O.; Akermark, B. *Angew. Chem., Int. Ed. Engl.* **1997**, *36*, 1723 and references therein.

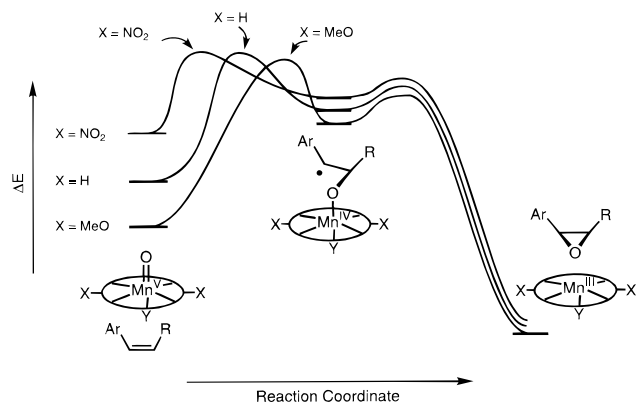
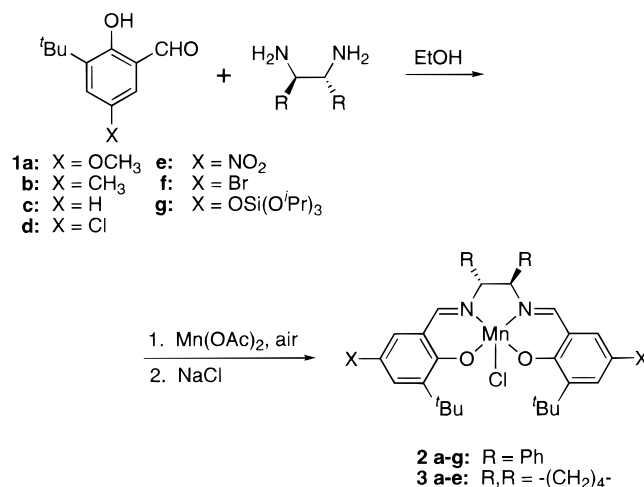


**Figure 1.** Schematic energy diagram illustrating the proposed effect of ligand substituents on the (salen)Mn-catalyzed epoxidation reaction. More electron-donating substituents stabilize the Mn(V)oxo relative to the Mn(IV) radical intermediate resulting in a later, more product-like transition state.

catalyzed epoxidation of *cis*-disubstituted olefins,<sup>9</sup> and since that discovery, the importance of electronic effects in asymmetric catalytic reactions has been increasingly appreciated.<sup>10</sup> In the case of the (salen)Mn-catalyzed epoxidation, electron-donating substituents on the ligand were found to lead to higher levels of asymmetric induction, while electron-withdrawing substituents led to decreased enantioselectivity. In the original report,<sup>9</sup> we suggested that these effects might be interpreted according to a Hammond Postulate argument, wherein ligand substituents influence enantioselectivity by modulating the reactivity of the high-valent (salen)Mn oxo intermediate. Thus, electron-withdrawing substituents were proposed to lead to a more reactive (salen)Mn oxo intermediate, which adds to olefin in a comparatively early transition state and affords lower levels of enantioselectivity; conversely, electron-donating groups attenuate the reactivity of the oxo species, leading to a comparatively late transition state and concomitantly higher enantioselectivity (Figure 1).

Herein we present a detailed analysis of these catalyst electronic effects. The diastereo- and enantioselectivities, kinetic isotope effects, and temperature profiles of the epoxidation reaction catalyzed by a series of substituted (salen)Mn com-

## Scheme 2



plexes provide strong support for the mechanistic interpretation represented schematically in Figure 1.

## Results and Discussion

**1. Correlation of Enantioselectivity and the Electronic Character of the Catalyst.** One of the appealing features of salen-based catalysts is that the ligands may be tuned both sterically and electronically in a synthetically straightforward manner by variation of the corresponding diamines and salicyl aldehyde ligand precursors (Scheme 2). While the first investigations on the (salen)Mn-catalyzed asymmetric epoxidation established that steric bulk at the 3,3'-position of the salen ligand was essential in order to achieve high enantioselectivities,<sup>11</sup> subsequent studies revealed that variations in the electronic properties of the substituents at the 5,5'-position of the catalysts can have an equally profound effect.<sup>9</sup>

To quantify the influence of the 5,5'-substituent on the enantioselectivity of the epoxidation reaction, we evaluated the catalysts depicted in Scheme 2 in the epoxidation of each of three model substrates: 2,2-dimethylchromene (**4**), a member of a synthetically important class of olefins that is epoxidized with particularly high enantioselectivity by (salen)Mn catalysts;<sup>12</sup> *cis*- $\beta$ -methylstyrene (**5**), an aryl-substituted alkene which is among the most commonly employed model substrates for enzymatic and nonenzymatic epoxidation systems; and *cis*-2,2-dimethyl-3-hexene (**6**), a nonconjugated olefin. Epoxidation of these alkenes under biphasic NaOCl conditions<sup>13</sup> revealed the same trend for each substrate, with electron-donating groups on the catalyst leading to higher enantioselectivities. The observed enantioselectivities correlated directly with the  $\sigma_p$  values of the 5,5'-substituents on the catalyst, as reflected in the Hammett plots in Figure 2.

Although the nature of the correlation was maintained for all three substrates, the magnitude of the dependence varied significantly: **6** undergoes epoxidation with low enantioselectivity (26–37% ee), whereas for **4** the observed ee ranges from 22% (catalyst **2e**) to 96% (catalyst **2a**).<sup>14</sup> This latter example corresponds to a remarkable difference between

(9) (a) Jacobsen, E. N.; Zhang, W.; Güler, M. L. *J. Am. Chem. Soc.* **1991**, *113*, 6703.

(10) (a) Rajanbabu, T. V.; Casalnuovo, A. L. *J. Am. Chem. Soc.* **1992**, *114*, 6262. (b) Inoguchi, K.; Sakuraba, S.; Achiwa, K. *Synlett* **1992**, 169. (c) Nishiyama, H.; Yamaguchi, S.; Kondo, M.; Itoh, K. *J. Org. Chem.* **1992**, *57*, 4306. (d) Nishiyama, H.; Yamaguchi, S.; Kondo, M.; Itoh, K. *J. Org. Chem.* **1992**, *57*, 4306. (e) Li, Z.; Conser, K. R.; Jacobsen, E. N. *J. Am. Chem. Soc.* **1993**, *115*, 5326. (f) Chang, S.; Heid, R. M.; Jacobsen, E. N. *Tetrahedron Lett.* **1994**, *35*, 669. (g) Rajanbabu, T. V.; Ayers, T. A.; Casalnuovo, A. L. *J. Am. Chem. Soc.* **1994**, *116*, 4101. (h) Mashima, K.; Kusano, K.; Sato, N.; Matsumura, Y.; Nozaki, K.; Kumobayashi, H.; Sayo, N.; Hori, Y.; Ishizaki, T.; Akutagawa, S.; Takaya, H. *J. Org. Chem.* **1994**, *59*, 3064. (i) Casalnuovo, A. L.; Rajanbabu, T. V.; Ayers, T. A.; Warren, T. H. *J. Am. Chem. Soc.* **1994**, *116*, 9869. (j) Rajanbabu, T. V.; Ayers, T. A. *Tetrahedron Lett.* **1994**, *35*, 4295. (k) Legros, J. Y.; Fiaud, J. C. *Tetrahedron* **1994**, *50*, 465. (l) Rajanbabu, T. V.; Casalnuovo, A. L. *Pure Appl. Chem.* **1994**, *7*, 1535. (m) Park, S. B.; Murata, K.; Matsumoto, H.; Nishiyama, H. *Tetrahedron: Asymmetry* **1995**, *6*, 2487. (n) Vander Velde, S. L.; Jacobsen, E. N. *J. Org. Chem.* **1995**, *60*, 5380. (o) Schnyder, A.; Hintermann, L.; Togni, A. *Angew. Chem., Int. Ed. Engl.* **1995**, *34*, 931. (p) Zhang, H. C.; Xue, F.; Mak, T. C. W.; Chan, K. S. *J. Org. Chem.* **1996**, *61*, 8002. (q) Gravert, D. J.; Griffin, J. H. *Inorg. Chem.* **1996**, *35*, 4837. (r) Rajanbabu, T. V.; Casalnuovo, A. L. *J. Am. Chem. Soc.* **1996**, *118*, 6325. (s) Halterman, R. L.; Jan, S. T.; Abdulwali, A. H.; Standlee, D. J. *Tetrahedron* **1997**, *53*, 11277. (t) Rajanbabu, T. V.; Ayers, T. A.; Halliday, G. A.; You, K. K.; Calabrese, J. C. *J. Org. Chem.* **1997**, *62*, 6012. (u) Reetz, M. T.; Waldvogel, S. R.; Goddard, R. *Tetrahedron Lett.* **1997**, *38*, 5967.

(11) Zhang, W.; Loebach, J. L.; Wilson, S. R.; Jacobsen, E. N. *J. Am. Chem. Soc.* **1990**, *112*, 2801.

(12) Lee, N. H.; Muci, A. R.; Jacobsen, E. N. *Tetrahedron Lett.* **1991**, *32*, 5053.

(13) Zhang, W.; Jacobsen, E. N. *J. Org. Chem.* **1991**, *56*, 2296.

(14) Katsuki has reported a case where a MeO-substituted chiral (salen)-Mn complex affords lower epoxidation enantioselectivity than the corresponding catalyst bearing a H-substituent: Hamada, T.; Fukuda, T.; Imanishi, H.; Katsuki, T. *Tetrahedron* **1996**, *52*, 515.

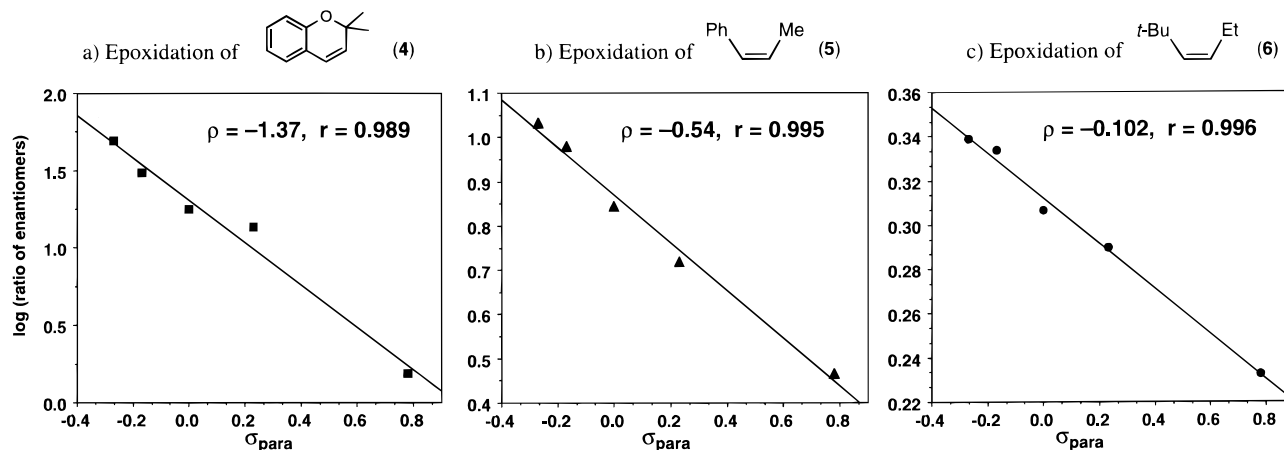


**Figure 2.** Correlation of the enantioselectivity of epoxidation of alkenes **4–6**—expressed as the log of the ratio of epoxide enantiomers—against  $\sigma_p$  values of the substituent X in catalysts **2a–e**.

diastereomeric transition state energies,  $\Delta\Delta G^\ddagger$ , of 2.0 kcal/mol. Catalysts **3a–e** display analogous trends, affording slightly higher enantioselectivities. For example, epoxidation of **4** afforded 66% ee with **3e** and 98% ee with **3a** ( $\Delta\Delta G^\ddagger = 2.0$  kcal/mol). The linearity of the correlations indicates that changes in enantioselectivity are indeed due to the electronic character of the catalysts and that the steric perturbations imposed by variation of the 5,5'-substituents do not play a significant role.

**2. Mechanistic Possibilities.** In principle, these sizable electronic effects may be ascribed to any of several factors. The 5,5'-substituent could induce significant conformational distortion of the reactive (salen)Mn(V) oxo intermediate. While this possibility is difficult to assess directly, since to date no (salen)-Mn(V) oxo species have yielded to structural characterization,<sup>15</sup> the X-ray crystal structures of a number of chiral (salen)Mn(III) catalysts indicate that the complexes maintain a square planar salen ligand conformation regardless of the electronic properties of the ligand substituents.<sup>16,17</sup> A second possibility is that the substituents may effect changes in the Mn–oxo bond length in the active species, in turn altering the nonbonding substrate/ligand interactions in the relevant transition states. However, such effects on metal–oxo bond length are typically small.<sup>18</sup> Further, the observed ee trend runs contrary to what one might predict from this hypothesis, since electron-withdrawing substituents should shorten the Mn–oxo bond length and thus lead to an increase, rather than a decrease, in the enantioselectivity of oxo transfer.

An alternative explanation is that the electronic effect on enantioselectivity derives from changes in the reactivity of the Mn(V) oxo intermediate imparted by the substituents on the

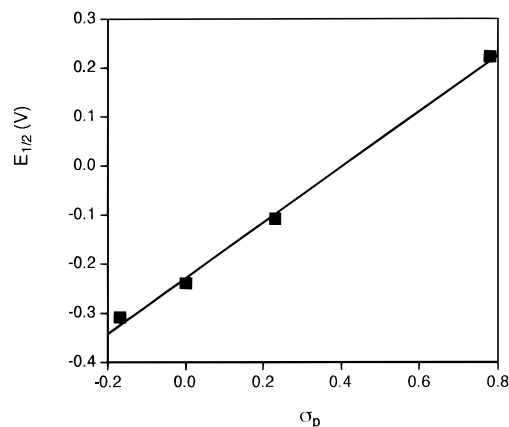


**Figure 3.** Plot of  $E_{1/2}$  for the Mn(II)/Mn(III) redox couple vs  $\sigma_p$  values of the substituent X in catalysts **3b–e**. The CV measurements were carried out at room temperature under argon: [complex] =  $10^{-3}$  M in  $\text{CH}_2\text{Cl}_2$ ;  $[\text{Bu}_4\text{NBF}_4] = 0.1$  M; scan speed 200 mV/s; working electrode, glassy carbon; auxiliary electrode, Pt wire; reference electrode, Ag/AgCl/KCl.

catalyst. Electron-donating substituents on the catalyst would be expected to stabilize the high-valent Mn(V) oxo intermediate, attenuating its reactivity and thus generating a relatively milder oxidant. Similarly, electron-withdrawing substituents on the catalyst are expected to destabilize the Mn(V) oxo intermediate, making it a more reactive oxidant.<sup>19</sup> The results of electrochemical studies on catalysts **3a–e** lend credence to this supposition: there is a clear correlation between  $\sigma_p$  of the 5,5'-substituent and the value of  $E_{1/2}$  for the Mn(II)/Mn(III) redox couple (Figure 3). Accurate measurement of the redox potentials for higher Mn oxidation states was prevented by the apparent instability of Mn(IV) and Mn(V) species under the electrochemical reaction conditions.

In accord with the Hammond postulate, a milder oxidant should lead to an oxygen transfer to alkene via a more product-

(15) For recent efforts directed toward the isolation of reactive Mn(V) oxo complexes, see: (a) Groves, J. T.; Lee, J.; Marla, S. S. *J. Am. Chem. Soc.* **1997**, *119*, 6269. (b) Feichtinger, D.; Plattner, D. A. *Angew. Chem., Int. Ed. Engl.* **1997**, *36*, 1718.

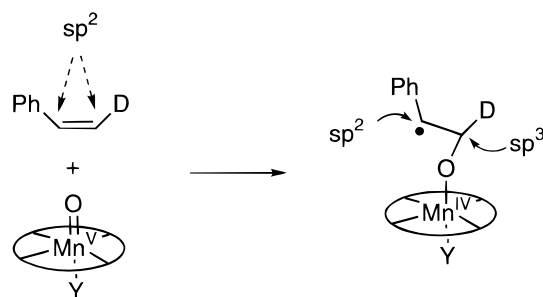
(16) Pospisil, P. J.; Carsten, D. H.; Jacobsen, E. N. *Chem. Eur. J.* **1996**, *2*, 974.

(17) Katsuki has demonstrated recently that sparteine can induce moderate enantioselectivity in the epoxidation of certain olefins catalyzed by achiral (salen)Mn complexes and has proposed a mechanism involving complexation of the amine to the catalyst resulting in a nonplanar reactive ligand conformation: Hashihayata, T.; Ito, Y.; Katsuki, T. *Tetrahedron* **1997**, *53*, 9541. However, the very low yields of epoxide obtained in these reactions (0.1–0.5 equiv relative to sparteine) raise the possibility that any enantioselectivity might be due instead to secondary reactions such as kinetic resolution of epoxide mediated by the chiral amine. This notion is supported by the fact that epoxide yields decrease and enantioselectivities increase with added amine or with added water in the presence of amine.

(18) Nugent, W. A.; Mayer, J. M. *Metal–Ligand Multiple Bonds*; Wiley: New York, 1988; pp 148–152.

(19) The most direct test of this hypothesis—direct comparison of the rates of reactions catalyzed by electron-rich and electron-poor catalysts—is precluded by the fact that mass transport of the aqueous oxidant into the organic layer is the rate-limiting step under biphasic conditions: Suárez, A.; Pospisil, P. J.; Jacobsen, E. N. Unpublished results. See also: (a) Senanayake, C. H.; Smith, G. B.; Liu, J.; Fredenburgh, L. E.; Ryan, K. M.; Hughes, D. L.; Larsen, R. D.; Verhoeven, T. R.; Reider, P. J. *Tetrahedron Lett.* **1995**, *36*, 3993. (b) Senanayake, C. H.; Smith, G. B.; Ryan, K. M.; Fredenburgh, L. E.; Liu, J.; Roberts, F.; Hughes, D. L.; Larsen, R. D.; Verhoeven, T. R.; Reider, P. J. *Tetrahedron Lett.* **1996**, *37*, 3271. (c) Hughes, D. L.; Smith, G. B.; Liu, J.; Dezeny, G. C.; Senanayake, C. H.; Larsen, R. D.; Verhoeven, T. R.; Reider, P. J. *J. Org. Chem.* **1997**, *62*, 2222.

## Scheme 3

**Table 1.** Epoxidation of *cis*- $\beta$ -Deuteriostyrene Catalyzed by **3a–e**

entry	catalyst	$k_H/k_D$	enantiofacial selectivity <sup>a</sup>	cis/trans <sup>a</sup>
1	<b>3a</b> (X = OMe)	0.82	5.4	5.1
2	<b>3b</b> (X = Me)	0.84	4.8	5.7
3	<b>3c</b> (X = H)	0.86	4.4	6.3
4	<b>3d</b> (X = Cl)	0.90	4.2	6.9
5	<b>3e</b> (X = NO <sub>2</sub> )	0.95	2.0	7.1

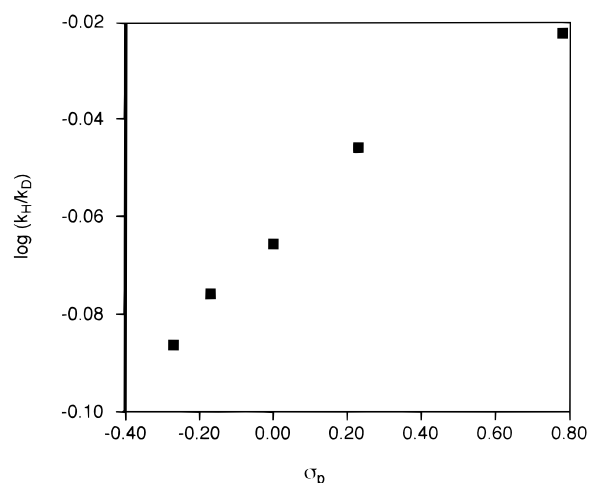
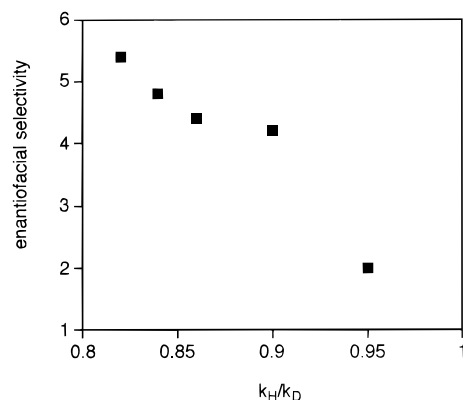
<sup>a</sup> Determined by <sup>1</sup>H NMR in the presence of chiral shift reagent (Eu(hfc)<sub>3</sub>) according to the following equation: enantiofacial selectivity = [cis + trans (major enantiomers)]/[cis + trans (minor enantiomers)]. See: Zhang, W.; Lee, N. H.; Jacobsen, E. N. *J. Am. Chem. Soc.* **1994**, *116*, 425.

like transition state. Since this transformation involves the encounter of two reactants which, at the origin of the reaction coordinate, do not interact at all, one might expect a higher degree of stereochemical communication in a later transition state. Oxo transfer from a more reactive oxidant, on the other hand, should proceed via a more reactant-like transition state, with greater spatial separation between substrate and catalyst and concomitantly poorer differentiation of the diastereomeric transition structures (Figure 1). As outlined in the following discussion, support for this mechanistic proposal has been provided through isotopic labeling studies and the temperature profile of the epoxidation.

**3. A. Correlation of Deuterium Isotope Effects with the Electronic Character of the Catalyst.** A direct evaluation of the relative position of the transition state on the reaction coordinate was obtained by competitive epoxidation of styrene and *cis*- $\beta$ -deuteriostyrene with catalysts **2a–e**. On transformation to the radical intermediate, the  $\beta$ -carbon of styrene undergoes a formal rehybridization from  $sp^2$  to  $sp^3$  which, in principle, should lead to the observation of an inverse secondary isotope effect ( $k_H/k_D < 1$ ) for the epoxidation (Scheme 3).<sup>20,21</sup> Further, the magnitude of  $k_H/k_D$  should vary in concert with the position of the transition state: later transition states, in which the  $\beta$ -carbon has more  $sp^3$  character, should exhibit smaller values of  $k_H/k_D$ . The experimental data reveal a direct correlation between  $k_H/k_D$  and  $\sigma_p$  (Table 1, Figure 4), indicating that the electronic character of the catalyst does indeed alter the degree of rehybridization at the  $\beta$ -carbon and thus the position of the transition state leading to formation of the radical intermediate. Perhaps more relevant, a direct correlation is observed between  $k_H/k_D$  and the enantioselectivity of epoxidation (Figure 5). This result supports in a compelling and quantitative manner the notion that the later the transition state in the first

(20) Isaacs, N. *Physical Organic Chemistry*, 2nd ed.; John Wiley & Sons: New York, 1995; pp 296–301.

(21) In contrast, there is no change in hybridization at the  $\alpha$  carbon. As would be expected, the experimentally determined kinetic isotope effect for the epoxidation of styrene vs  $\alpha$ -deuteriostyrene,  $k_H/k_D = 1$ . It should be noted that this observation is inconsistent with a mechanism for epoxidation involving oxametallacycle formation. See refs 8a and 8e.

**Figure 4.** Correlation of the kinetic isotope effect in the epoxidation of styrene vs *cis*- $\beta$ -deuteriostyrene as a function of the  $\sigma_p$  values of the substituent X in catalysts **3a–e**.**Figure 5.** Correlation of the enantiofacial selectivity in the first C–O bond-forming step in the epoxidation of *cis*- $\beta$ -deuteriostyrene with the kinetic isotope effect using catalysts **3a–e**.

C–O bond-forming step, the higher the enantioselectivity in the epoxidation reaction.

**3. B. Electronic Effects on Cis/Trans Partitioning.** As an additional mechanistic handle provided by the isotope labeling study outlined above, the *cis*/*trans* partitioning in the second C–O bond-forming step could be assessed directly by measuring the relative proportions of *cis*- and *trans*- $\beta$ -deuteriostyrene oxide produced. The *cis*/*trans* ratio represents relative rate of the collapse and rotation/collapse pathways outlined in Scheme 1 (eq 1), in turn reflecting the energetic barrier to ring closure. A higher barrier should lead to a longer lived radical intermediate, and thus a greater extent of rotational isomerization and a lower *cis*/*trans* ratio.

$$k_{cis}/k_{trans} = (\% \text{ cis epoxide})/(\% \text{ trans epoxide}) \quad (1)$$

A correlation was revealed between  $k_{cis}/k_{trans}$  and  $\sigma_p$  (Table 1, Figure 6) wherein electron-poor catalysts lead to higher *cis*/*trans* ratios relative to catalysts bearing electron-rich substituents. This observed effect can be rationalized in a straightforward manner: as ring closure of the radical intermediate to generate the second C–O bond of the epoxide occurs with formal reduction of Mn(IV) to Mn(III), this process should be favored by more electron-withdrawing substituents on the metal ligand, leading to an increase in the *cis*/*trans* ratio relative to more electron-rich ligands. Thus, the electronic character of the (salen)Mn epoxidation catalysts has been demonstrated to

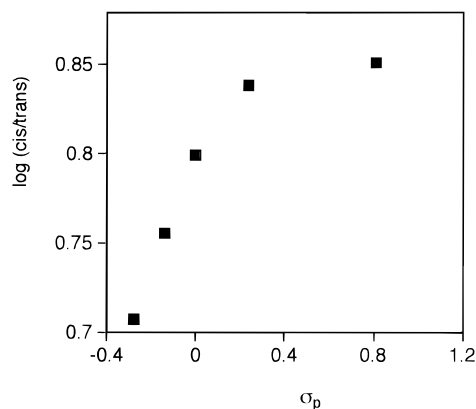


**Figure 6.** Correlation between the cis/trans product ratio in the epoxidation of *cis*- $\beta$ -deuteriostyrene and the  $\sigma_p$  values of the substituent X in catalysts **3a–e**.

influence both formation and ring closure of the radical intermediate and consequently affect the stereoselectivity of both C–O bond-forming steps in the oxygen-atom-transfer process.

**3. C. Temperature Effects in the Epoxidation.** We have recently developed an anhydrous, low-temperature protocol for the (salen)Mn-catalyzed epoxidation reaction employing the combination of *m*-chloroperbenzoic acid (*m*-CPBA) and *N*-methylmorpholine *N*-oxide (NMO) as the terminal oxidant system.<sup>22</sup> These reactions are monophasic, anhydrous, and homogeneous, allowing access to a broader temperature range for the epoxidation. With the ability to carry out epoxidations at  $-78$  °C, significant improvements in the enantiomeric excesses have been attained for many substrates, most notably terminal olefins such as styrene.<sup>22b</sup> In addition, it has become possible to evaluate the temperature-dependence of enantioselectivity for (salen)Mn-catalyzed epoxidations, allowing further insight into the nature of the electronic effect.

The epoxidation of indene was carried out under low-temperature conditions with catalysts **2a–c,e,f**. Indene is epoxidized without partitioning to *cis* and *trans* diastereomers, and as such the observed ee is directly representative of the inherent facial selectivity of the first C–O bond-forming step, as long as this first step is completely irreversible (eq 2).<sup>23</sup>

$$\text{enantiofacial selectivity} = k_{\text{major}}/k_{\text{minor}} = (\% \text{ major epoxide})/(\% \text{ minor epoxide}) \quad (2)$$

The relationship between enantioselectivity in the epoxidation of indene under the *m*-CPBA conditions and the  $\sigma_p$  values of the 5,5'-substituents of different catalysts was investigated over a range of different temperatures (Figure 7). The Hammett plot at each temperature is linear, consistent with the results obtained in the epoxidations of **4–6** at room temperature using NaOCl as the terminal oxidant. A notable feature of this temperature profile is the existence of an "isoelectronic point"—a single point at or near which all of the Hammett plots intersect—in analogy to the well-established isokinetic effect.<sup>24</sup> The isokinetic effect is characterized by the intersection at a single point (the isokinetic point) of the Eyring plots for a series of related

(22) (a) Palucki, M.; Pospisil, P. J.; Zhang, W.; Jacobsen, E. N. *J. Am. Chem. Soc.* **1994**, *116*, 9333. (b) Palucki, M.; McCormick, G. J.; Jacobsen, E. N. *Tetrahedron Lett.* **1996**, *37*, 5457.

(23) This assumption is based on the general observation that conjugated *cis*-alkenes are observed not to undergo *cis/trans* isomerization under the conditions of epoxidation.

(24) (a) Isaacs, N. *Physical Organic Chemistry*, 2nd ed.; John Wiley & Sons: New York, 1995; pp 116–7. (b) Leffler, J. E.; Grunwald, E. *Rates and Equilibria in Organic Reactions*; Wiley: New York, 1963.

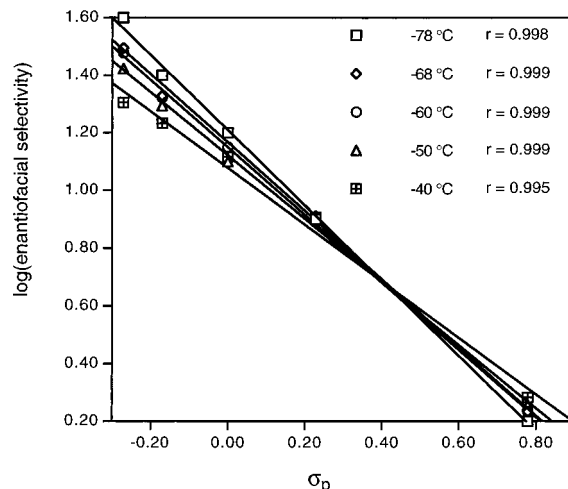


**Figure 7.** Correlation between the enantioselectivity in the epoxidation of indene at various temperatures with the  $\sigma_p$  values of the substituent X in catalysts **2a–c** and **2e–g**.

reactions. The observation of an isokinetic relationship is generally taken as evidence that the reaction parameter being varied (e.g., temperature, solvent, or, in this case,  $\sigma_p$ ) is influencing only one type of interaction in the system. The isoelectronic relationship seen in the present case may thus be taken as evidence that variation of the electronic nature of the 5,5'-substituents of the ligand influences only one central aspect of the reaction, namely the degree of the first C–O bond formation and thus the position of the enantiodifferentiating transition state along the reaction coordinate.

As noted earlier, direct kinetic analysis of the biphasic epoxidation reaction is complicated by the zero-order rate dependence on olefin that results from rate-limiting transfer of oxidant into the organic layer.<sup>19c</sup> Although it was hoped that the single-phase *m*CPBA/NMO conditions would be more amenable to the measurement of absolute rate constants, epoxidations of indene carried out at  $-78$  °C were, remarkably, typically complete within 1 min, again precluding straightforward rate measurements.<sup>25</sup> Making the conservative estimate that  $t_{1/2} = 30$  s and applying the Eyring equation to the rate expression in eq 3,<sup>26</sup> this places an upper limit of ca. 12–13 kcal/mol on  $\Delta G^\ddagger$  at [indene] = 1 M, testifying to the very high reactivity of the (salen)Mn oxo intermediate.<sup>15</sup>

$$\text{rate} = [(\text{salen})\text{Mn}(\text{V})\text{oxo}][\text{indene}] \quad (3)$$

Analysis of the temperature dependence of the observed enantioselectivities (Figure 8) provided a means of evaluating  $\Delta\Delta H^\ddagger$  and  $\Delta\Delta S^\ddagger$  for the two diastereomeric transition states leading to formation of the major and minor enantiomeric indene oxide products (Table 2). Two opposing trends emerge on inspection of these data. The enthalpic contribution ( $\Delta\Delta H^\ddagger$ ) dominates in the more enantioselective reactions effected by catalysts bearing electron-rich substituents. Conversely, the enthalpic contribution diminishes and the entropic contribution ( $\Delta\Delta S^\ddagger$ ) becomes more important with more electron-withdrawing catalyst substituents, to the point where, for the nitro-substituted catalyst **2e**, the enthalpic component marginally favors the minor enantiomer, but is overcome by the entropic contribution. This latter case leads to an unusual situation in

(25) Efforts to lower the observed rate of epoxidation by effecting the reactions under high dilution conditions were thwarted by the observation of low catalyst turnovers under these conditions.

(26) In this analysis, [(salen)Mn(V)oxo] is taken to be equal to the initial catalyst concentration.

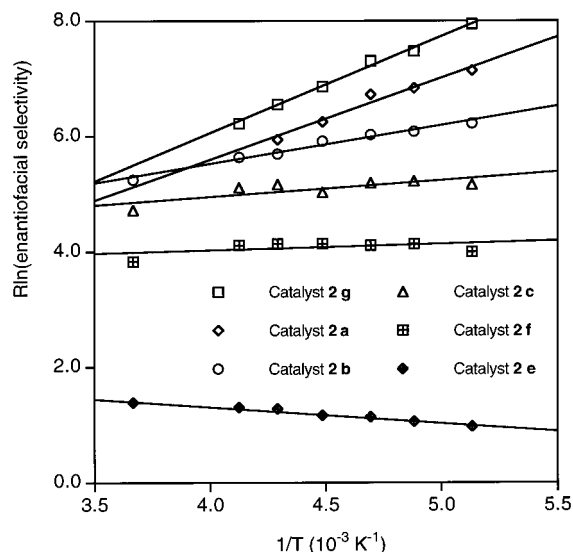


**Figure 8.** Eyring plots for the epoxidation of indene with catalysts 2a–c and 2e–g.

**Table 2.** Relative Activation Parameters for the Formation of Indene Oxide Enantiomers Catalyzed by Complexes 2a–c, e–g

entry	catalyst	substituent	$\Delta\Delta H^\ddagger$ (kcal mol <sup>-1</sup> )	$\Delta\Delta S^\ddagger$ (cal mol <sup>-1</sup> K <sup>-1</sup> )
1	2g	OSi( <i>i</i> Pr) <sub>3</sub>	1.70 ± 0.08	−0.69 ± 0.35
2	2a	OCH <sub>3</sub>	1.40 ± 0.16	−0.07 ± 0.76
3	2b	CH <sub>3</sub>	0.66 ± 0.05	2.90 ± 0.21
4	2c	H	0.29 ± 0.10	3.80 ± 0.44
5	2f	Br	0.11 ± 0.09	3.60 ± 0.40
6	2e	NO <sub>2</sub>	−0.28 ± 0.02	2.50 ± 0.10

which the observed degree of asymmetric induction increases, rather than decreases, with increasing temperature.

The straightforward correlation between the relative activation parameters for the diastereomeric transition states and the electronic properties of the catalysts appears to be quite consistent with the Hammond postulate arguments presented above. If electron-donating substituents do indeed lead to a later transition state with a more highly developed C–O bond, the energetic differences between the diastereomeric transition states should be more dependent on the degree of bond formation (reflected by  $\Delta\Delta H^\ddagger$ ). Similarly, in the case of electron-deficient catalysts, if the transition state is earlier, less ordered, and characterized by a lower degree of C–O bond formation, it is reasonable for whatever enantioselectivity that is observed to derive primarily from entropic factors.

## Conclusions

A wide range of experimental data support the proposal that the electronic character of chiral (salen)Mn catalysts influences the enantioselectivity of the catalytic epoxidation by altering the position of the transition state in the first C–O bond-forming step. The critical experimental results are as follows:

(a) Linear Hammett plots correlating enantioselectivity in the epoxidation of *cis* disubstituted olefins with the  $\sigma_p$  values of the 5,5'-substituents on the catalyst.

(b) Secondary deuterium isotope effects correlating the value of  $k_H/k_D$  at C<sub>β</sub>, and thus the degree of rehybridization, with both  $\sigma_p$  and the observed enantioselectivity.

(c) Linear Hammett plots correlating enantioselectivity in the epoxidation of indene with  $\sigma_p$  over a 100 °C temperature range, including the observation of an "isoelectronic" point indicating that a single reaction parameter (such as the degree of bond

formation and thus transition state position) is influenced by the 5,5'-substituent.

(d) Eyring analyses revealing that enantioselectivity in epoxidations with the most selective catalysts relies almost entirely on enthalpic factors, while less enantioselective catalysts are subject to greater entropic influence.

The notion that the position of the transition state along the reaction coordinate is the critical element in the (salen)Mn-catalyzed asymmetric epoxidation reaction is perhaps quite reasonable in retrospect, but it could hardly have been anticipated in the initial design of these systems. It seems likely that (salen)Mn-catalyzed epoxidations are not the only reactions that can exhibit a correlation between enantioselectivity and the position of the enantioselectivity-determining step along the reaction coordinate. The observations made in this study may therefore hold general implications for the design of asymmetric catalysts, particularly those that proceed without substrate precoordination.

## Experimental Section

**General.** Enantiomeric ratios measured by HPLC were determined using the Daicel Chiralcel O-series column with a mobile phase of 10% isopropyl alcohol in hexane unless otherwise noted. Tetrahydrofuran (THF), diethyl ether, benzene, and toluene were distilled from the sodium benzophenone ketyl. Dichloromethane, hexane, and acetonitrile were distilled from calcium hydride. All other reagents and solvents were reagent grade and were used without further purification unless otherwise specified. 4-Methylmorpholine *N*-oxide (NMO) and indene were obtained from Aldrich Chemical Co. and were used as received. *m*-Chloroperbenzoic acid was purified according to the literature procedure.<sup>27</sup>

**General Procedure for the Epoxidation of Indene.** A solution of indene (24 μL, 0.20 mmol), NMO (117 mg, 1.00 mmol), and catalyst 2a (7.7 mg, 0.01 mmol) in 2 mL of dry CH<sub>2</sub>Cl<sub>2</sub> was cooled to the appropriate temperature for 10 min before the addition of solid *m*-CPBA (72 mg, 0.40 mmol). After stirring for 1 h at the appropriate temperature, 4 mL of 3 N NaOH and 2 mL of H<sub>2</sub>O were added to the solution. The organic phase was separated, washed with 4 mL of brine, and dried over Na<sub>2</sub>SO<sub>4</sub>. Removal of the drying agent followed by concentration yielded the epoxide which was dissolved in hexane and filtered through a pad of Celite. Complete removal of the solvent from the resulting filtrate provided indene oxide (96% ee, 95% yield) that was >95% pure by GC and <sup>1</sup>H NMR analysis. <sup>1</sup>H NMR (CDCl<sub>3</sub>) δ 2.97 (dd, 1H, *J* = 3.0, 17.7 Hz), 3.21, (d, 1H, *J* = 18.0 Hz), 4.13 (t, *J* = 2.7 Hz), 4.26, (d, 1H, *J* = 2.7 Hz), 7.10–7.30 (m, 3H), 7.50 (d, 1H, *J* = 6.9 Hz).

**General Procedure for the Epoxidation of *cis*-β-Deuteriostyrene.** To a solution of *cis*-β-deuteriostyrene (0.30 mmol), catalyst (8 mol %), in 1 mL of CH<sub>2</sub>Cl<sub>2</sub> was added a solution 0.55 M buffered bleach (pH = 11.3, 1.50 mL, 0.90 mmol) at room temperature. The mixture was stirred for 1 h before the addition of 2 mL of H<sub>2</sub>O and 2 mL of CH<sub>2</sub>Cl<sub>2</sub>. The organic layer was separated, washed with brine (3 mL), and dried over Na<sub>2</sub>SO<sub>4</sub>. Removal of the drying agent and solvent followed by chromatography (SiO<sub>2</sub>) afforded pure *cis*-β-deuteriostyrene oxide (78% yield).

**General Procedure for the Measurement of the Kinetic Inverse Isotope Effect.** To a solution of *cis*-β-deuteriostyrene (1 equiv), styrene (1 equiv), and catalyst (4 mol %) in CH<sub>2</sub>Cl<sub>2</sub> was added buffered bleach (0.2 equiv) at room temperature. The mixture was allowed to stir for 1 h before the addition of 2 mL of H<sub>2</sub>O and 2 mL of CH<sub>2</sub>Cl<sub>2</sub>. The organic layer was separated, washed with brine (3 mL), and dried over Na<sub>2</sub>SO<sub>4</sub>. GC and <sup>1</sup>H NMR analysis of the reaction mixture provided a measure of the relative rates of epoxidation for styrene and *cis*-β-deuteriostyrene.

**Preparation of Chiral Ligands and the Corresponding (salen)-Mn(III) Complexes.** Catalysts 2e–f, 3a–c, and their ligand precursors

(27) Bortolini, O.; Campestrini, S.; DiFuria, F.; Modena, G. *J. Org. Chem.* 1987, 52, 3.

were have been reported previously.<sup>16,28</sup> The synthesis and characterization of ligand precursors to **2a–d** and **3d–e** are provided as Supporting Information.

**Chloro-(R,R)-[[2,2'-(1,2-diphenyl-1,2-ethanediyl)bis(nitrilomethylidene)]bis[4-methoxy-6-(1,1-dimethylethyl)phenolato]]-N,N',O,O']-manganese(III) (2a).** A three-necked round-bottom flask equipped with a reflux condenser, an addition funnel, and a septum was charged with the salen ligand (1.00 g, 1.69 mmol) and 100 mL of EtOH. The mixture was heated to reflux, and a solution of Mn(OAc)<sub>2</sub>·4H<sub>2</sub>O dissolved in 5 mL of H<sub>2</sub>O was added whereupon the solution immediately turned brown. After 30 min of reflux, air was bubbled into the solution and refluxed for an additional 30 min. Brine (3 mL) was added and the mixture allowed to cool to room temperature. The solvents were removed under vacuum, and then 100 mL of CH<sub>2</sub>Cl<sub>2</sub> was added. The solution was washed with 100 mL of brine and 100 mL of H<sub>2</sub>O and dried over anhydrous Na<sub>2</sub>SO<sub>4</sub>. Removal of the drying agent followed by concentration of filtrate resulted in a brown powder which was chromatographed (EtOH/CH<sub>2</sub>Cl<sub>2</sub>) to afford the catalyst (0.882 g, 54% yield) as a brown solid. IR (KBr) 3281, 2942, 1605, 1541, 1454, 1418, 1350, 1296, 1206, 1156, 1057, 818 cm<sup>-1</sup>; mp 282.5–283 °C; HRMS (FAB) *m/z* calcd (C<sub>38</sub>H<sub>42</sub>ClMnN<sub>2</sub>O<sub>4</sub>) 680.2214, found 680.2212.

**Chloro-(R,R)-[[2,2'-(1,2-diphenyl-1,2-ethanediyl)bis(nitrilomethylidene)]bis[4-methyl-6-(1,1-dimethylethyl)phenolato]]-N,N',O,O']-manganese(III) (2b).** To a solution of the salen ligand (561 mg, 1.00 mmol) in 10 mL of 95% EtOH was added dropwise a solution of Mn(OAc)<sub>2</sub>·4H<sub>2</sub>O (490 mg, 2.00 mmol) dissolved in 5 mL of 95% EtOH. The resulting brown solution was heated at reflux for 30 min before the addition of a solution of LiCl (212 mg, 5.00 mmol) in 5 mL of EtOH was added. The mixture was heated at reflux for an additional 30 min. Water (5 mL) was added, and the mixture was cooled slowly to room temperature. The precipitate was collected by filtration to afford the brown catalyst (564 mg, 87% yield): IR (KBr) 2952, 1615, 1539, 1454, 1429, 1343, 1310, 1235, 1204, 1169, 1005, 855, 822, 700 cm<sup>-1</sup>; mp 279–280 °C; HRMS (FAB) *m/z* calcd (C<sub>38</sub>H<sub>42</sub>ClMnN<sub>2</sub>O<sub>2</sub>) 648.2315, found 648.2320. Anal. Calcd for C<sub>38</sub>H<sub>42</sub>ClMnN<sub>2</sub>O<sub>2</sub>: C, 70.31; H, 6.52; N, 4.32; Cl, 5.46; Mn, 8.46. Found: C, 70.30; H, 6.53; N, 4.22; Cl, 5.59; Mn, 8.28.

**Chloro-(R,R)-[[2,2'-(1,2-diphenyl-1,2-ethanediyl)bis(nitrilomethylidene)]bis[6-(1,1-dimethylethyl)phenolato]]-N,N',O,O']-manganese(III) (2c).** To a hot solution of the salen ligand precursor to **2c** (2.644 g, 5.0 mmol) in 100 mL of 95% EtOH was added Mn(OAc)<sub>2</sub>·4H<sub>2</sub>O (2.451 g, 10.00 mmol) as a solid in one portion. The mixture was heated to reflux for 30 min under an atmosphere of air and then cooled to room temperature. A solution of LiCl (1.060 g, 25.00 mmol) in EtOH (20 mL) was added, and the mixture was heated to reflux for an additional 30 min. The mixture was allowed to cool to room temperature, affording 2.365 g of product as dark brown crystals. A second crop of product (0.490 g) was obtained by adding H<sub>2</sub>O to the filtrate (total yield 91%): mp 271.5–272 °C; IR (KBr) 2950, 1593, 1543, 1414, 1389, 1302, 1196, 1145, 870 cm<sup>-1</sup>; HRMS (FAB) *m/z* calcd (C<sub>36</sub>H<sub>38</sub>ClMnN<sub>2</sub>O<sub>2</sub>) 620.2002, found 620.1999. Anal. Calcd for C<sub>36</sub>H<sub>38</sub>ClMnN<sub>2</sub>O<sub>2</sub>: C, 68.62; H, 6.24; N, 4.45; Cl, 5.63; Mn, 8.72. Found: C, 68.45; H, 6.43; N, 4.15; Cl, 5.87; Mn, 8.66.

**Chloro-(R,R)-[[2,2'-(1,2-diphenyl-1,2-ethanediyl)bis(nitrilomethylidene)]bis[4-chloro-6-(1,1-dimethylethyl)phenolato]]-N,N',O,O']-manganese(III) (2d).** To a hot solution of the salen ligand precursor to **2d** (0.602 g, 1.0 mmol) in 40 mL of 95% EtOH was added Mn(OAc)<sub>2</sub>·4H<sub>2</sub>O (0.490 g, 2.00 mmol) as a solid in one portion. The reaction mixture turned brown immediately. The mixture was heated to reflux for 30 min under an atmosphere of air and then cooled to room temperature. A solution of LiCl (0.212 g, 5.00 mmol) in EtOH (20 mL) was added, and the mixture was heated to reflux for an additional 30 min. Water (10 mL) was added until no more precipitate formed. The resulting brown solid was collected by filtration, washed with 20 mL of 30% EtOH, and dried in air to give 0.628 g of product (91% yield): mp 297.5–298 °C; IR (KBr) 2950, 2868, 1613, 1534, 1495, 1454, 1426, 1404, 1389, 1304, 1173, 1005, 816 cm<sup>-1</sup>; HRMS (FAB)

*m/z* calcd (C<sub>36</sub>H<sub>36</sub>Cl<sub>3</sub>MnN<sub>2</sub>O<sub>2</sub>) 688.1223, found 688.1220. Anal. Calcd for C<sub>36</sub>H<sub>36</sub>Cl<sub>3</sub>MnN<sub>2</sub>O<sub>2</sub>: C, 62.67; H, 5.26; N, 4.06; Cl, 15.41; Mn, 7.96. Found: C, 62.98; H, 5.28; N, 4.08; Cl, 15.38; Mn, 7.92.

**Chloro-(R,R)-[[2,2'-(1,2-diphenyl-1,2-ethanediyl)bis(nitrilomethylidene)]bis[4-(triisopropylsiloxy)-6-(1,1-dimethylethyl)phenolato]]-N,N',O,O']-manganese(III) (2g).** To a solution of diphenylethylenediamine (244 mg, 1.15 mmol) in 90 mL of EtOH was added 3-*tert*-butyl-5-(triisopropylsiloxy)salicylaldehyde<sup>16</sup> (800 mg, 2.30 mmol). The resulting yellow solution was heated to reflux for 25 min before the addition of a solution of Mn(OAc)<sub>2</sub>·4H<sub>2</sub>O (0.564 g, 2.30 mmol) in 5 mL of H<sub>2</sub>O. The resulting brown solution was heated to reflux for 30 min, after which air was bubbled through the solution via a needle for an additional 30 min. Brine (5 mL) was added, and the mixture was further heated at reflux for 30 min before being cooled to ambient temperature. The solvent volume was reduced to ca. 15 mL under vacuum, and CH<sub>2</sub>Cl<sub>2</sub> (100 mL) and water (100 mL) were added. The organic phase was separated, washed with brine (100 mL), and dried over Na<sub>2</sub>SO<sub>4</sub>. After solvent removal, the residue was purified by chromatography (SiO<sub>2</sub>, 5% EtOH/CH<sub>2</sub>Cl<sub>2</sub>) to afford 0.854 g of product (77% yield): mp 280–280.8 °C; IR (CH<sub>2</sub>Cl<sub>2</sub>) 2947, 2868, 1600, 1535, 1464, 1409, 1343, 1230, 1041, 1010, 963, 882, 869 cm<sup>-1</sup>; HRMS (FAB) *m/z* calcd (C<sub>54</sub>H<sub>78</sub>ClMnN<sub>2</sub>O<sub>4</sub>Si<sub>2</sub>) 929.4881 (M – Cl<sup>+</sup>), found 929.4914.

**Chloro-(R,R)-[[2,2'-(1,2-cyclohexanediyl)bis(nitrilomethylidene)]bis[4-nitro-6-(1,1-dimethylethyl)phenolato]]-N,N',O,O']-manganese(III) (3d).** A three-necked round-bottom flask equipped with a reflux condenser, an addition funnel, and a septum was charged with the ligand precursor to **3d** (0.413 g, 0.815 mmol) and 60 mL of EtOH. The mixture was heated to reflux and a solution of Mn(OAc)<sub>2</sub>·4H<sub>2</sub>O (0.400 g, 1.630 mmol) dissolved in 5 mL of H<sub>2</sub>O was added, whereupon the solution immediately turned brown. After the mixture was heated to reflux for 30 min, air was bubbled into the solution and reflux was continued for an additional 30 min. Brine (3 mL) was added, and the mixture was allowed to cool to room temperature. Solvents were removed under vacuum, and the residue was dissolved in 100 mL of CH<sub>2</sub>Cl<sub>2</sub>. The solution was then washed with 100 mL of brine and 100 mL of H<sub>2</sub>O and dried over anhydrous Na<sub>2</sub>SO<sub>4</sub>. Removal of the drying agent followed by concentration of the filtrate resulted in a brown powder which was purified by chromatography (5% EtOH/CH<sub>2</sub>Cl<sub>2</sub>), affording the product (0.482 g, 84% yield): mp 338–339 °C; IR (CCl<sub>4</sub>) 2965, 2949, 2284, 2249, 2245, 1618, 1593, 1536, 1410, 1332, 1307, 1265, 1175, 771, 752, 745 cm<sup>-1</sup>; HRMS (FAB) *m/z* calcd (C<sub>28</sub>H<sub>34</sub>Cl<sub>2</sub>MnN<sub>4</sub>O<sub>2</sub>) 555.1378 (M – Cl<sup>+</sup>), found 555.1368.

**Chloro-(R,R)-[[2,2'-(1,2-cyclohexanediyl)bis(nitrilomethylidene)]bis[4-nitro-6-(1,1-dimethylethyl)phenolato]]-N,N',O,O']-manganese(III) (3e).** A three-necked round-bottom flask equipped with a reflux condenser, an addition funnel, and a glass stopper was charged with the salen ligand (0.209 g, 0.400 mmol) and 20 mL of EtOH. The mixture was heated to reflux, and a solution of Mn(OAc)<sub>2</sub>·4 H<sub>2</sub>O dissolved in 2 mL of 50% EtOH/H<sub>2</sub>O was added whereupon the solution immediately turned brown. After 30 min of refluxing, 1 mL of brine was added and the resulting solution refluxed for an additional 30 min. After the mixture was cooled to room temperature, the solvents were removed and 50 mL of CH<sub>2</sub>Cl<sub>2</sub> was added. The solution was then washed with 50 mL of brine followed by 50 mL of H<sub>2</sub>O and dried over anhydrous Na<sub>2</sub>SO<sub>4</sub>. Removal of the drying agent followed by concentration of the filtrate resulted in a brown powder which was chromatographed (5% EtOH/CH<sub>2</sub>Cl<sub>2</sub>), affording the product (0.220 g, 90% yield): IR (CCl<sub>4</sub>) 2955, 1628, 1598, 1565, 1510, 1330, 1311, 1296, 1271, 1116, 706, 698, 690 cm<sup>-1</sup>; mp >400 °C; HRMS (FAB) *m/z* calcd (C<sub>28</sub>H<sub>34</sub>ClMnN<sub>4</sub>O<sub>6</sub>) 577.1859 (M – Cl<sup>+</sup>), found 577.1849.

**Acknowledgment.** This work was supported by the NIH (GM43214) and by a postdoctoral fellowship to N.S.F. (NIGMS).

**Supporting Information Available:** Synthesis and characterization of the ligand precursors to **2a–d** and **3d–e** (4 pages). See any current masthead page for ordering and Internet access instructions.

(28) Larrow, J. R.; Jacobsen, E. N.; Gao, Y.; Hong, Y.; Nie, X.; Zepp, C. M. *J. Org. Chem.* **1994**, 59 1938.